Vibration Suppression Control for an Articulated Robot: Effects of Model-Based Control Applied to a Waist Axis

Masahiko Itoh and Hiroshi Yoshikawa

Abstract: This paper deals with a control technique of eliminating the transient vibration of a waist axis of an articulated robot. This technique is based on a model-based control in order to establish the damping effect on the mechanical part. The control model is related to the velocity control loop, and it is composed of reduced-order electrical and mechanical parts. Using this model, the velocity of the load is estimated, which is converted to the motor shaft. The difference between the estimated load speed and the motor speed is calculated dynamically, and it is added to the velocity command to suppress the transient vibration of a waist axis of the robot arm. The function of this technique is to increase the cut-off frequency of the system and the damping ratio at the driven machine part. This control model is easily obtained from design or experimental data and its algorithm can be easily installed in a DSP. This control technique is applied to a waist axis of an articulated robot composed of a harmonic drive gear reducer and a robot arm with 5 degrees of freedom. Simulations and experiments show satisfactory control results to reduce the transient vibration at the end-effector.

Keywords: Servomechanism, geared system, robot arm, vibration control, model-based control.

1. INTRODUCTION

Most of the industrial robots have the geared reduction mechanisms between output shafts of motors and driven machine parts, namely the power transmission systems. For instance, spur gears, harmonic drive gear reducers, RV gear reducers and so on are well known. The insufficiency of the torsional stiffness of the geared reduction mechanism often induces transient vibrations mainly related to the eigenvalues of the mechanical parts in the lower-frequency range when the motor starts or stops. This transient vibration causes a problem such that the tact time of the system may be lengthened.

To solve this problem, the full-closed loop control which feeds back the state variables measured with sensors at the end effectors [1], the state-feedback control using observers [2, 3], the velocity feedback control with a disturbance observer [4] and the dynamic damper comprised of the software [5] have been proposed. However, the full-closed loop control technique and the control technique using an additional sensor are hard to set up in reality and incur increasing the cost. Further, the conventional observer technique to suppress the transient vibration requires a precise model of the mechanical system and an additional low-pass filter in a compensating loop. As a result, the observer technique has difficulties in setting up and adjusting its parameters in the field.

On the other hand, one of the authors had proposed a simple and easily realizable technique for eliminating the transient vibration of a drum driving servo system [6]. This system is a typical example of the geared mechanical system such that the stiffness of the geared stage is much higher than those of a shaft, a coupling, and a timing belt. The proposed technique is based on a model-based control. The control model is related to the velocity control loop, and it is composed of reduced-order electrical and mechanical parts by considering that the transient vibration which should be eliminated is mainly dominated by the first vibration mode of the geared mechanical system. This model calculates the rotational speed of the driven machine part, which is converted to the motor shaft. The difference between the calculated rotational speed of the driven machine part and the motor speed is calculated dynamically, and it is added to the velocity command to suppress

Manuscript received April 20, 2002; revised June 24, 2003; accepted July 21, 2003. Recommended by Editor Keum-shik Hong.

Masahiko Itoh is with the Department of Mechanical Engineering, Miyagi National College of Technology, 48 Nodayama Shiote, Medeshima, Natori-shi, Miyagi 981-1239, Japan (e-mail: itoh@miyagi-ct.ac.jp).

Hiroshi Yoshikawa is with the Control Systems Division, Sanyo Denki Co., Ltd., 1-15-1 Kita-Otsuka, Toshima-ku, Tokyo 170-8451, Japan (e-mail: hiroshi_yoshikawa@sanyodenki.co.jp).

the transient vibration generated at the drum after being multiplied by a gain. The function of this technique is to establish a damping effect without a response time-lag at the driven machine part.

The effectiveness of the model-based control mainly depends on the value of the gain. In [6], this technique is applied to the case such that the inertia ratio of the driven machine part to the driving machine part is less than 1.0 and the value of the gain is positive. Simulations and experiments showed satisfactory control results in reducing the transient vibration.

The control model is easily obtained from design or experimental data. Its algorithm can be easily installed in a DSP. In addition, parameters of the control model are easily adjusted in the field.

In this paper, the proposed model-based control technique is applied to a waist axis of a robot system which is composed of a motor, a harmonic drive gear reducer and a robot arm with 5 degrees of freedom. This case is a typical example such that the inertia ratio is greater than 1.0 and the value of the gain is negative. Simulations and experiments on the time responses show satisfactory control results in reducing the transient vibration of the robot arm. As a result, the settling time can be shortened down to about 1/2 of the uncompensated vibration level.

2. REDUCED-ORDER MODEL OF AN ARTICULATED ROBOT SYSTEM

2.1. Equations of motion

As a typical example of the robot system, an articulated robot shown in Fig. 1 is taken up. This system can be regarded as a 3-mass system composed of a motor rotor, a gear reducer's input shaft and a driven machine part, and it is controlled by the velocity control loop using the PI control.

Equations of motion of this geared system are written as

$$J_m\ddot{\theta}_m + C_s(\dot{\theta}_m - \dot{\theta}_g) + K_s(\theta_m - \theta_g) = T_m, \quad (1)$$

$$J_g\ddot{\theta}_g + C_s(\dot{\theta}_g - \dot{\theta}_m) + K_s(\theta_g - \theta_m) + \{C_g(\dot{\theta}_g/R_g - \dot{\theta}_l) + K_g(\theta_g/R_g - \theta_l)\}/R_g = 0, \quad (2)$$

$$J_l\ddot{\theta}_l + C_g(\dot{\theta}_l - \dot{\theta}_g/R_g) + K_g(\theta_l - \theta_g/R_g) = 0, \quad (3)$$

where

θ_m = angular rotation of the motor,
θ_g = angular rotation of the gear reducer's input shaft,
θ_l = angular rotation of the driven machine part,
T_m = output torque of the motor,
J_m = moment of inertia of the motor rotor,
J_g = moment of inertia of the reducer's input shaft,
J_l = moment of inertia of the driven machine part,
R_g = reduction ratio of the gear reducer,
K_s = torsional stiffness between the motor rotor and the gear reducer's input shaft,
K_g = torsional stiffness of the gear reducer,
C_s = damping factor between the motor rotor and the gear reducer's input shaft,
C_g = damping factor of the gear reducer.

Further, when the motor speed is controlled by the PI control, equations related to the motor armature are expressed as

$$L\frac{di}{dt} = K_c(K_v e + \frac{K_v}{T_i}\int e dt - K_{cb} i) - Ri - K_e\omega_m, \quad (4)$$

$$e = \omega_{cmd} - \omega_m. \quad (5)$$

The output torque of the motor is expressed as

$$T_m = K_t i, \quad (6)$$

where

ω_{cmd} = velocity command,
ω_m = rotating speed of the motor,
ω_g = rotating speed of the gear reducer's input shaft = rotating speed of the wave generator,
ω_l = rotating speed of the driven machine part,
e = error,
i = current of the armature,
R = motor armature resistance,
L = motor armature inductance,
K_t = torque constant,
K_e = voltage constant,
K_c = current loop gain,
K_{cb} = current feedback gain,
K_v = proportional gain of the PI control,
T_i = integral time constant of the PI control.

According to (1)-(6), a block diagram of the geared mechanical system can be expressed as Fig. 2.

2.2. Reduced-order model of mechanical part

Most of the geared mechanical systems can be grouped into two classes due to the insufficiency of the torsional stiffness. The first case is that the stiffness of a geared stage is much higher than those of shafts.

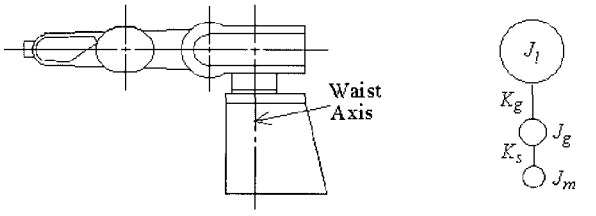

(a) Robot arm. (b) Model.

Fig. 1. A robot arm and its analytical model.

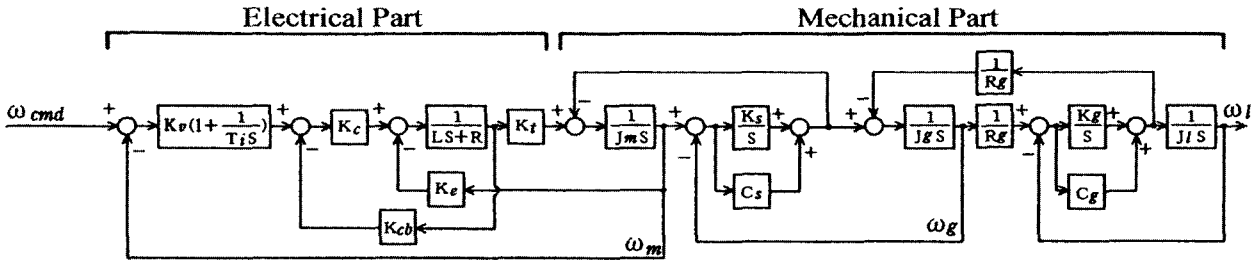

Fig. 2. Block diagram of a waist axis of an articulated robot.

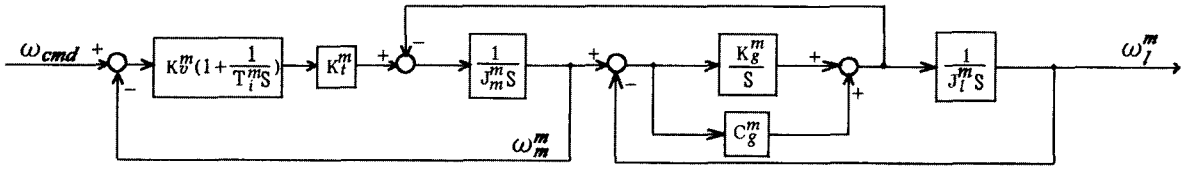

Fig. 3. Block diagram of reduced-order system.

The second case is that the stiffness of a geared stage is much lower than that of a driven machine part such that a rigid body is directly connected to the reducer's output shaft. This articulated robot system can be regarded as the second case.

Consequently, this paper deals with a case such that the residual vibration is mainly dominated by the first vibration mode and the higher order vibration modes are apart from the first one. As a result, the 3-mass system shown in Fig. 2 is transformed into a 2-mass system shown in Fig. 3 by considering only the first vibration mode. In this reduced-order model, the natural angular frequency ω_n and the damping ratio γ_n are expressed as

$$\omega_n = \sqrt{K_g{}^m (1/J_m{}^m + 1/J_l{}^m)}, \tag{7}$$

$$\gamma_n = \frac{C_g{}^m (1/J_m{}^m + 1/J_l{}^m)}{2\omega_n}, \tag{8}$$

where

$$J_m{}^m = J_m + J_g, \tag{9}$$

$$J_l^m = J_l / R_g^2, \tag{10}$$

$$K_g{}^m = K_g / R_g^2, \tag{11}$$

$$C_g{}^m = C_g / R_g^2. \tag{12}$$

Here, the superscript "m" shows that parameters belong to the model. Defining the inertia ratio R_n as $R_n = J_l^m / J_m{}^m$ and transforming (7) and (8), J_l^m, $K_g{}^m$ and $C_g{}^m$ are expressed as

$$J_l^m = R_n J_m{}^m, \tag{13}$$

$$K_g{}^m = \frac{R_n J_m{}^m}{1+R_n} \omega_n{}^2, \tag{14}$$

$$C_g{}^m = \frac{2R_n J_m{}^m}{1+R_n} \gamma_n \omega_n. \tag{15}$$

Using this expression, the reduced order model can be easily obtained from not only design data but also measured data.

2.3. Reduced-order model of electrical part

Next, a reduced order electrical model can be obtained. Here, the effect of the counter electromotive force is ignored. Further, the next two items are considered.

1) The angular cut-off frequency ω_c of the current control loop is much higher than the first natural angular frequency of the mechanical system.

2) The current loop gain within ω_n is about 1.0. Therefore, the current control system composed of the current control loop and the torque constant is expressed as a proportional gain K_t^m. As a result, a simplified PI control system is obtained as shown in Fig. 3. Expressing the natural angular frequency ω_e and the damping ratio of the electrical part as (16) and (17) respectively, the parameters of reduced-order model can be easily adjusted.

$$\omega_e = \sqrt{\frac{K_v{}^m K_t{}^m}{T_i{}^m J_m{}^m}}, \tag{16}$$

$$\zeta_e = \frac{1}{2}\sqrt{\frac{T_i{}^m K_v{}^m K_t{}^m}{J_m{}^m}}, \tag{17}$$

where $K_v{}^m = K_v$ and $T_i{}^m = T_i$.

3. MODEL-BASED CONTROL

3.1. Control system

Fig. 4 shows the block diagram of the model-based control system related to the velocity control loop.

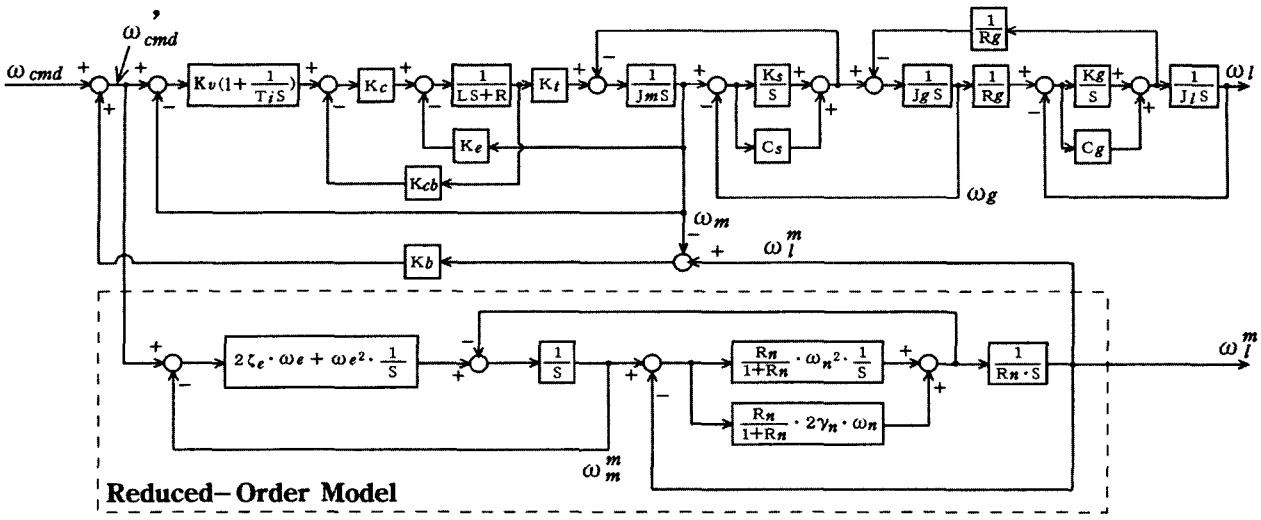

Fig. 4. Block diagram of model-based control.

Using the relationship of (7)-(17), the block diagram of the reduced-order model shown in Fig. 3 is trans formed into the dotted-line part of Fig. 4. The purpose of the model-based control is to suppress the residual vibration dominated by the first vibration-mode of the mechanical system.

In the compensating control system, the difference between the load's speed ω_l^m which is estimated at the motor shaft and the motor speed ω_m is dynamically calculated, and it is multiplied by the gain K_b. Finally, $K_b(\omega_l^m - \omega_m)$ is added to the velocity command ω_{cmd} as follows:

$$\omega'_{cmd} = \omega_{cmd} + K_b(\omega_l^m - \omega_m). \tag{18}$$

3.2. Stability

Table 1 shows conditions for simulations. The first natural frequency of the mechanical system varies from 7Hz to12Hz depending on the arm's posture as shown in Fig. 5. In Fig. 5, N.F. is shortened form of Natural Frequency. L1 and L2 represent the rotating radius of the end-effector with respect to the waist axis for Posture1 and Posture2, respectively.

In the simulations, the stability is considered by calculating the loci of system eigenvalues when the value of K_b is changed from 0.0 to -1.0. To obtain the system eigenvalues, first the model-based control system shown in Fig. 4 is re-expressed using the state variable approach, and then the eigenvalues of the system matrix are calculated.

Fig. 6 shows the loci of system eigenvalues. In this figure, eigenvalues of -11±47j and -16±73j are related to the first natural frequency of the torsional vibration for Posture1 and Posture2, respectively. Fig. 6 indicates that the control system is stable on the condition of $-0.9 \le K_b \le 0.0$.

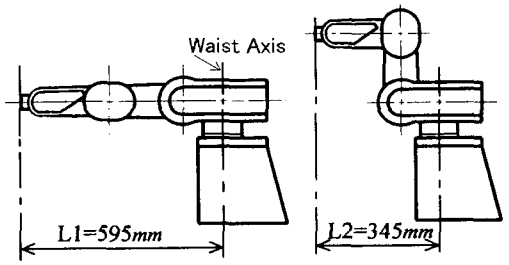

(a) Posture1 (N.F.=7Hz). (b) Posture2 (N.F.=12Hz).

Fig. 5. Correlation of natural frequency with the posture.

Table 1. Simulation and experimental conditions.

Parameter			Value	Unit
Moment of inertia		J_m	1.362×10^{-5}	kg·m^2
		J_g	2.048×10^{-5}	
	Posture1	J_l	2.852	
	Posture2	J_l	1.205	
Torsional stiffness		K_s	889.6	N·m/rad
		K_g	6967.3	
Damping coefficient		C_s	0.0137	N·m·s/rad
		C_g	22.553	
Gear reducer Reduction ratio		R_g	100	–
Velocity loop gain		K_v	0.15	A/(rad/s)
Integral time constant		T_i	1.0	s
Torque constant		K_t	0.316	N·m/A
Voltage constant		K_e	0.316	V/(rad/s)
Phase resistance		R	4.5	Ω
Phase inductance		L	0.0189	H
Current loop gain		K_c	118.84	V/A
Current feedback gain		K_{cb}	1.0	–
Feedback gain		K_b	0 or -0.7	–
Reduced-order model				
Electrical part				
Natural frequency		ω_e	188.4	rad/s
Damping ratio		ζ_e	1.0	–
Mechanical part				
Natural Freq.	Posture1	ω_n	151.2	rad/s
	Posture2	ω_n	163.3	
Damping ratio		γ_n	0.7	–
Inertia ratio	Posture1	R_n	8.363	–
	Posture2	R_n	3.256	

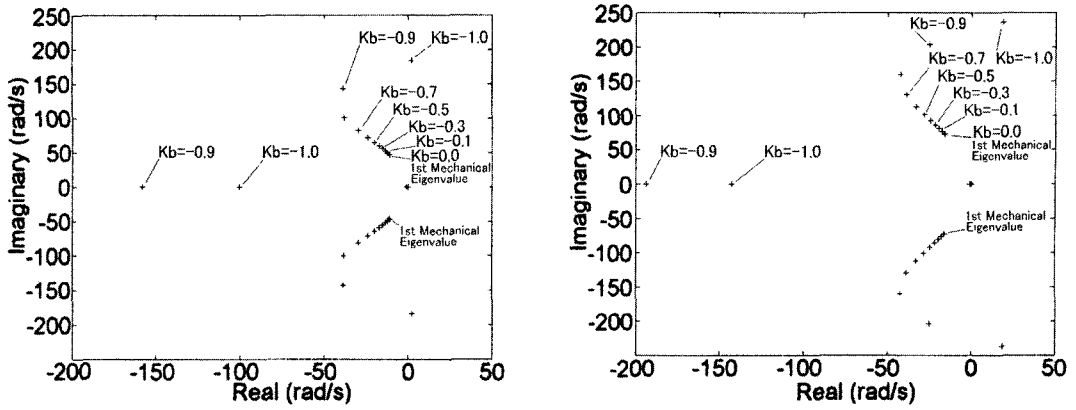

(a) In the case of Posture1 (N.F.=7Hz). (b) In the case of Posture2 (N.F.=12Hz).

Fig. 6. Loci of system eigenvalues.

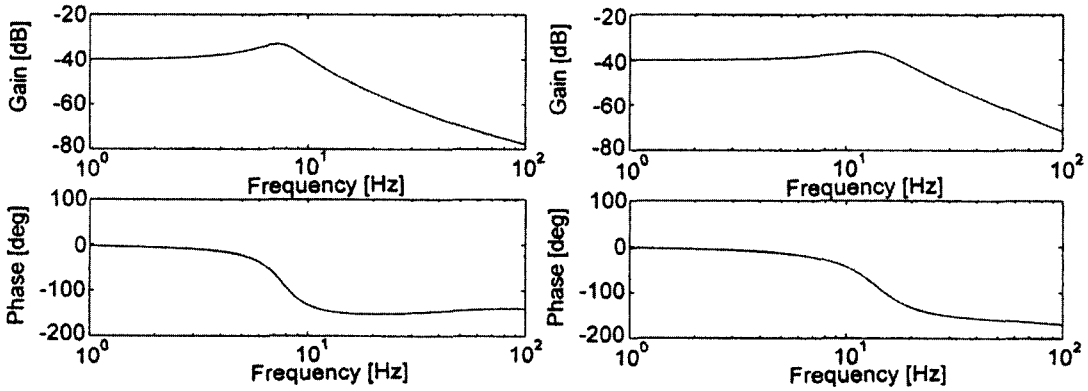

(a) Without model-based control. (b) With model-based control.

Fig. 7. Simulation results of ω_l/ω_{cmd} in the case of Posture1.

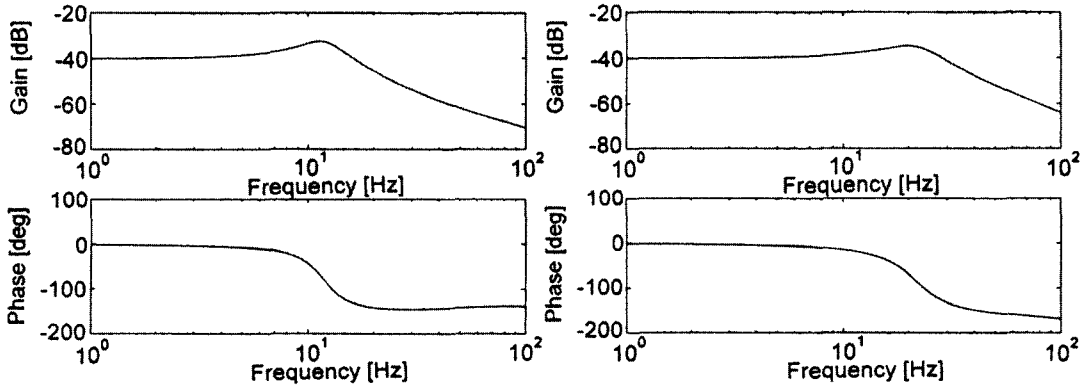

(a) Without model-based control. (b) With model-based control.

Fig. 8. Simulation results of ω_l/ω_{cmd} in the case of Posture2.

3.3. Simulation of frequency response

Fig. 7 and Fig. 8 show the Bode plots of the transfer function ω_l/ω_{cmd}. In these simulations, K_b is set to -0.7 after considering simulation results of the stability. These figures indicate that the proposed model-based control equivalently increases the cut- off frequency of the system and the damping ratio between the reducer's input shaft and the driven machine part.

3.4. Simulation of time response

Then, the time response is calculated by the Runge-Kutta method in order to verify the suppression effect on the residual vibration. Fig. 9 and Fig. 10 show simulation results. In these figures, *Arm accel.* represents the vibration acceleration in the direction of rotation at the point of L1 or L2 in Fig. 5.

In these simulations, a trapezoidal velocity profile is assigned. The constant acceleration in the start phase is 1000 min^{-1}/28 ms. The cruise velocity is 2000 min^{-1}. The constant deceleration in the arrival

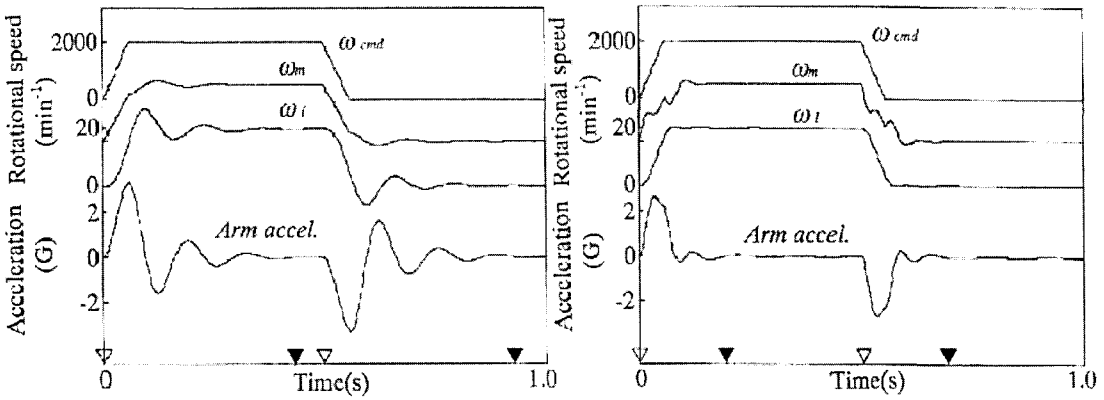

(a) Without model-based control. (b) With model-based control.

Fig. 9. Simulation results in the case of Posture1.

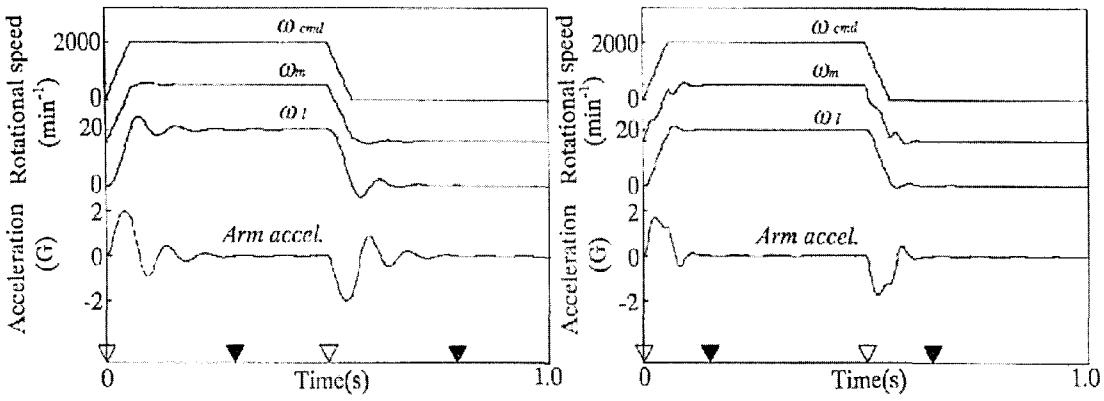

(a) Without model-based control. (b) With model-based control.

Fig. 10. Simulation results in the case of Posture2.

phase is -1000 min^{-1}/28 ms. The value of K_b is set to -0.7.

Fig. 9 indicates that the proposed model-based control suppresses the residual vibration of the end-effector in view of the vibration acceleration. The settling time, namely the time interval between ∇ and ▼, is reduced down to about 1/2 (from 432 to 193 ms) without the time-delay of the load's response. Further, Fig. 10 indicates that the settling time is reduced down to about 1/2 (from 289 to 151 ms).

4. EXPERIMENTAL RESULTS AND CONSIDERATIONS

4.1. Experimental set-up

Fig. 11 shows a schematic diagram of the experimental set-up. Physical parameters of the experimental set-up are shown in Table 1. A harmonic drive gear reducer whose reduction ratio is 1/100 is connected to a motor, and a driven machine part is connected to this reducer's output shaft. The inertia ratios of the driven machine part to the driving machine part are about 8.4 for Posture1 and 3.3 for Posture2, respectively. The first natural frequency of the system varies from 7 Hz to 12 Hz depending on the posture of the robot arm as shown in Fig. 5.

With respect to the servo control system of the waist axis, an AC servo motor and a driver are employed. Their servo parameters are equivalently converted into those of the DC servo system as shown in Table 1.

4.2. Construction of control system

The velocity control system of the main control loop consists of the software servo system. The velocity command is generated from the personal computer.

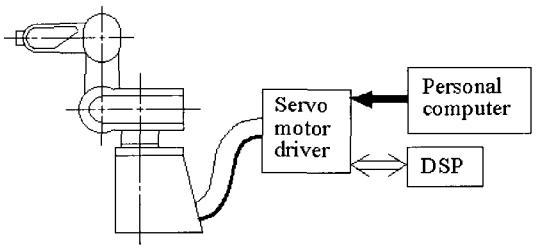

Fig. 11. Schematic diagram of the experimental set-up.

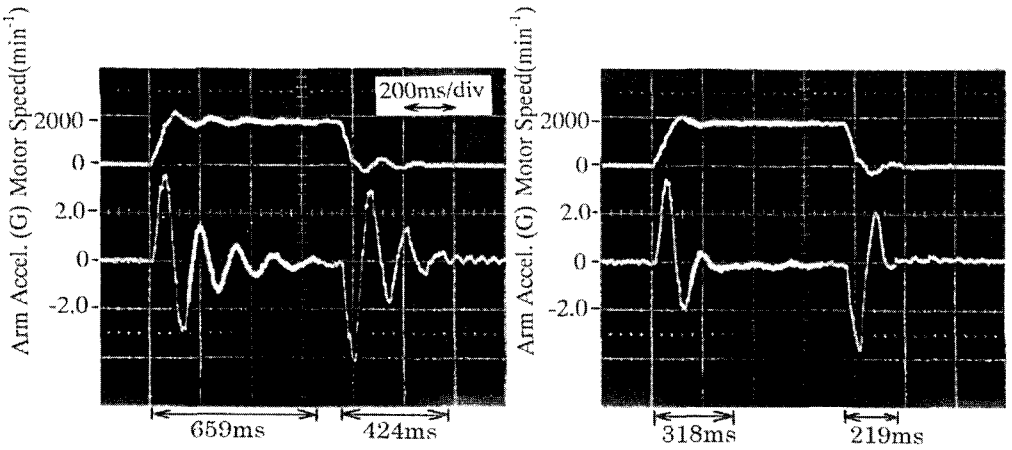

(a) Without model-based control. (b) With model-based control.

Fig. 12. Experimental results in the case of Posture1.

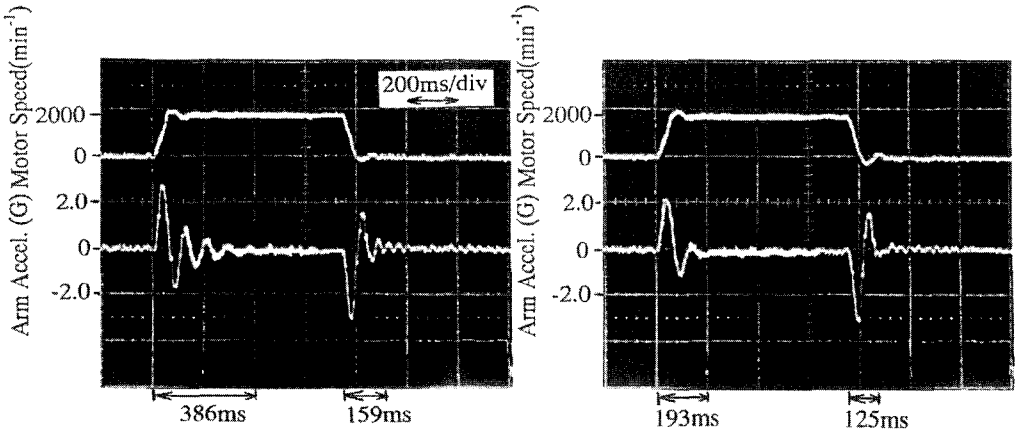

(a) Without model-based control. (b) With model-based control.

Fig. 13. Experimental results in the case of Posture2.

The sampling period of the main control loop is 0.4ms.

On the other hand, the compensating loop composed of a reduced-order model is installed in a DSP (Texas Instruments: TMS320C25) via the redesign after the simulation (e.g., [7]). The sampling period of this compensating loop is 1.2 ms, namely 3 times 0.4 ms. The first stage of 0.4 ms of the sampling period is assigned to the data input process from the servo motor driver. The second stage is assigned to the operation of the model-based control algorithm. The third stage is also assigned to the data output process to the servo motor driver. The value of K_b is set to -0.7 according to the simulation results of the time responses.

4.3. Effects on residual vibration

In experiments, a trapezoidal velocity profile is assigned in the same condition of the simulation. The constant acceleration in the start phase is 1000 min^{-1}/ 28 ms. The cruise velocity is 2000 min^{-1}. The constant deceleration in the arrival phase is -1000 min^{-1}/28 ms. To evaluate the suppression effects on the residual vibration in the direction of rotation, a piezoelectric accelerometer is attached to the end-effector. The motor speed and the vibration acceleration at the end-effector are measured with an oscilloscope.

Fig. 12 shows the suppression effect on the residual vibration in the case of Posture1. Fig. 12 shows that the settling time can be shortened down to about 1/2 (starting: from 659 to 318 ms, stopping: from 424 to 219 ms) by using the proposed model-based control.

Besides, Fig. 13 shows the suppression effect on the residual vibration in the case of Posture 2. Fig. 13 shows that the settling time can be shortened down to about 1/2 (starting: from 386 to 193 ms) by using the proposed model-based control.

5. CONCLUSIONS

A model-based control has been proposed as a technique of eliminating the residual vibration generated at a final stage of loading. This control model is

composed of electrical and mechanical parts of the velocity control loop. This control model can be obtained from design or experimental data. In addition, its algorithm is easily installed in a DSP.

In the previous study [6], the proposed model-based control was applied to a drum driving servo system, and the effectiveness of this technique was verified. This case is a typical example such that the inertia ratio of the driven machine part to the driving machine part is less than 1.0, and the value of the gain K_b for the model-based control is positive.

In this paper, this control technique is applied to a waist axis of an articulated robot which is composed of a harmonic drive gear reducer whose reduction ratio is 1/100. This case is a typical example such that the inertia ratio of the driven machine part to the driving machine part is greater than 1.0, and the value of the gain K_b is negative. Simulations and experiments on the time responses show satisfactory control results in reducing the transient vibration of the end-effector. In other words, the settling time can be shortened down to about 1/2 of the uncompensated level.

REFERENCES

[1] S. Futami, N. Kyura, and S. Hara, "Vibration absorption control of industrial robots by acceleration feedback," *IEEE Trans. on Industrial Electronics*, vol. 30, no. 3, pp. 299-305, August 1983.

[2] K. Yuki, T. Murakami, and K. Ohnishi, "Vibration control of a 2-mass resonant system by the resonance ratio control," *Trans. IEE Japan*, vol. 113(D), no. 10, pp. 1162-1169, 1993 (In Japanese).

[3] K. Honke, Y. Inoue, Y. Nishida, and T. Nishimura, "Motion and vibration control for robot arm with elastic joint (application of disturbance observer including elastic vibration)," *Trans. Jpn. Soc. Mech. Eng.*, vol. 60(C), no. 577, pp. 3045-3050, 1994 (In Japanese).

[4] I. Godler, K. Ohnishi, and T. Yamashita, "Vibration suppression for a speed control system with gear," *Journal of the Jpn. Soc. Precision Eng.*, vol. 60, no. 1, pp. 86-90, 1994 (In Japanese).

[5] H. Sakuta, Y. Toshitani, and T. Yonezawa, "Vibration absorption control of robot arm by software servomechanism (2nd report)," *Trans. Jpn. Soc. Mech. Eng.*, vol. 54(C), no. 497, pp. 217-220, 1988 (In Japanese).

[6] M. Itoh and S. Kasei, "Suppression of transient vibration for geared mechanical system (effects of model-based control)," *Trans. Jpn. Soc. Mech. Eng.*, vol. 64(C), no. 623, pp. 2596-2601, 1998 (In Japanese).

[7] T. Mita, *Introduction to Digital Control*, Corona Publishing, pp.115-118, 1989 (In Japanese).

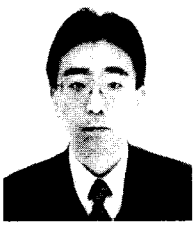

Masahiko Itoh received the B.S. and the M.S. degrees in Mechanical Engineering from the Tohoku University at Sendai, Japan, in 1986 and 1988, respectively. In 1988, he served as a research engineer for Sanyo Denki Co., Ltd. He received the Ph.D. degree in Mechanical Engineering from the Shinshu University at Nagano, Japan, in 1998. Since 2001, he has been with the Department of Mechanical Engineering at the Miyagi National College of Technology, Natori, Japan, where he is currently an Associate Professor. His research interests include mechatronics, vibration control, and robotics.

Hiroshi Yoshikawa received the B.S. degree in communications and Mechanical Engineering from the University of Electro-Communications in 1966. He joined Industrial Research Institute of Kanagawa in 1966. He joined Amada Co., Ltd. in 1982. In 1997, he joined Sanyo Denki Co., Ltd. as a senior engineer. His research interests include mechatronics, PC-based controller design, and networking controller design.